Published by Avanti Publishers

Journal of Advances in Applied & Computational Mathematics

ISSN (online): 2409-5761

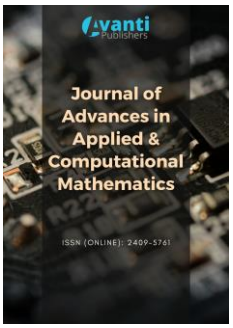

Semantic Segmentation to Extract Coronary Arteries in Invasive Coronary Angiograms

Chen Zhao[1], Robert Bober[2], Haipeng Tang[3], Jinshan Tang[4], Minghao Dong[5], Chaoyang Zhang[3], Zhuo He[1], Michele L. Esposito[6], Zhihui Xu[7,*], Weihua Zhou[1,8,*]

[1]*Department of Applied Computing, Michigan Technological University, Houghton, MI, 49931, USA*
[2]*Department of Cardiology, Ochsner Medical Center, New Orleans, LA, 70121, USA*
[3]*School of Computing Sciences and Computer Engineering, University of Southern Mississippi, Hattiesburg, MS, 39406, USA*
[4]*Department of Health Administration and Policy, George Mason University, Fairfax, VA, 22030, USA*
[5]*School of Computer and Communication Engineering, Zhengzhou University of Light Industry, Zhengzhou, Henan, China*
[6]*Department of Cardiology, Tufts Medical Center, Boston, MA, 02111, USA*
[7]*Department of Cardiology, The First Affiliated Hospital of Nanjing Medical University, Nanjing, China*
[8]*Center for Biocomputing and Digital Health, Institute of Computing and Cyber-systems, and Health Research Institute, Michigan Technological University, Houghton, MI, 49931, USA*

ARTICLE INFO

Article Type: Research Article

Keywords:
Binary Vascular Tree
Support Vector Machine
Coronary Artery Disease
Image Semantic Segmentation
Invasive Coronary Angiography

Timeline:
Received: March 22, 2022
Accepted: May 10, 2022
Published: May 24, 2022

Citation: Zhao C, Bober R, Tang H, Tang J, Dong M, Zhang C, He Z, Esposito ML, Xu Z, Zhou W. Semantic Segmentation to Extract Coronary Arteries in Invasive Coronary Angiograms. J Adv App Comput Math. 2022; 9: 76-85.

DOI: https://doi.org/10.15377/2409-5761.2022.09.6

ABSTRACT

Accurate semantic segmentation of each coronary artery using invasive coronary angiography (ICA) is important for stenosis assessment and coronary artery disease (CAD) diagnosis. In this paper, we propose a multi-step semantic segmentation algorithm based on analyzing arterial segments extracted from ICAs. The proposed algorithm firstly extracts the entire arterial binary mask (binary vascular tree) using a deep learning-based method. Then we extract the centerline of the binary vascular tree and separate it into different arterial segments. Finally, by extracting the underlying arterial topology, position, and pixel features, we construct a powerful coronary artery segment classifier based on a support vector machine. Each arterial segment is classified into the left coronary artery (LCA), left anterior descending (LAD), and other types of arterial segments. The proposed method was tested on a dataset with 225 ICAs and achieved a mean accuracy of 70.33% for the multi-class artery classification and a mean intersection over union of 0.6868 for semantic segmentation of arteries. The experimental results show the effectiveness of the proposed algorithm, which provides impressive performance for analyzing the individual arteries in ICAs.

*Corresponding Author
Email: wx_xzh@njmu.edu.cn and whzhou@mtu.edu
Tel: (+86)02568303120 and 906-487-2666

1. Introduction

Coronary artery disease (CAD) is the leading cause of morbidity and mortality in the United States and costs about 350 billion dollars annually [1]. Invasive coronary angiography (ICA) remains the gold standard for diagnosing CAD [2]. ICA involves the injection of contrast media into the epicardial arteries with the acquisition of continuous fluoroscopy. Detection of CAD is performed by visually comparing diseased arterial segments to normal arterial segments and is essential for the diagnosis and treatment.

Semantic segmentation of coronary vessels is extremely important for clinical decisions regarding mechanical revascularization. For these clinical decisions, automatic identification of correct anatomical branches provides meaningful information for automatic diagnosis report generation and region of interest visualization [3]. Meanwhile, successfully detecting the percent stenosis of a coronary artery improves diagnostic efficiency and confidence and influences management [4]. However, due to the overlap of arteries on ICA and the inter-subject variation of coronary artery segments, identifying the arterial branch is challenging. According to prior knowledge [5], the left main coronary artery (LMA) is the artery that arises from the aorta above the left cusp of the aortic valve and perfuses the anterior, septal, and lateral walls of the left ventricle. The LMA branches into the left anterior descending artery (LAD), which courses between the left and right ventricles towards the apex along the anterior interventricular sulcus, and the left circumflex artery (LCX) which courses laterally along the atrioventricular groove. Typically, practitioners analyze the entire vascular tree according to the position and morphology of LMA, LAD, and LCX.

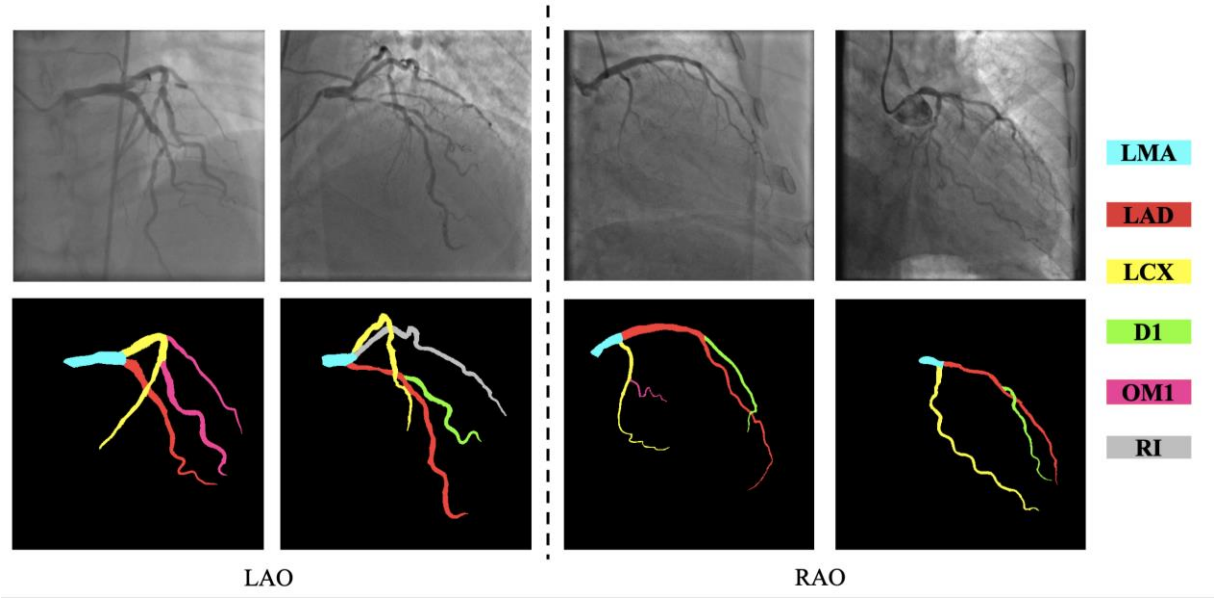

Figure 1: Illustration of semantic segmentation of arteries in (a) Left Anterior Oblique (LAO) view and (b) Right Anterior Oblique (RAO) view. For each view, the raw image and semantic maps are juxtaposed vertically. Arteries with different colors in the semantic maps represent different types of arteries.

Recently, deep learning techniques, especially variants based on convolutional neural networks (CNN), have been employed in coronary artery segmentation in ICAs. Nasr-Esfahani *et al*. [6] implemented a CNN which contained two convolutional layers to predict the patched arterial binary mask. The same group also used a CNN to classify the central pixel within the cropped patches into arterial pixel or background [7]. The AngioNet employed the DeepLabV3+ network as the backend for coronary artery segmentation and achieved a Dice score of 0.864 [8]. Our recent published network [9], feature pyramid U-Net++, was developed based on U-Net++ and integrated the feature pyramids to capture feature maps from different scales; the proposed network achieved a Dice score of 0.8899 on our dataset with 314 annotated coronary arteries.

However, due to the morphological similarity of different arteries, it is challenging for pixel-intensity-based models to discern each arterial segment and generate semantic segmentation. The inter-class difference of pixel

features between the arterial segments is difficult to be distinguished. Thus, the common deep learning models for nature image semantic segmentation tasks cannot achieve satisfying performance on artery semantic segmentation [10]. Xian *et al*. proposed a robust method for main coronary artery segmentation using four fully convolutional networks [11]. The designed model only identified the main coronary arteries on ICAs; however, the model cannot assess the arterial anatomy. Yang *et al*. trained a set of CNNs to achieve semantic segmentation [12]. Each CNN was a binary segmentation model which labeled only one type of the coronary artery segment, such as LCX and LAD. The designed method did not fully utilize the topological information from the vascular tree, and the most frequent errors were caused by mask separation and the overlap of the catheters. The coronary artery semantic segmentation integrating both topological and pixel-level features is still under study.

The topology is an important factor in arterial identification, which inspires us to convert arteries and their connections into graphs. The topological features, such as the node degrees, can be combined with the pixel-derived features in the semantic segmentation. The problem of semantic segmentation here will be converted into a problem that classifies the type of an unlabeled arterial segment. Figure **2** illustrates our overall workflow. In this paper, we propose a new machine learning-based approach to extract individual coronary arteries from ICAs by incorporating global position, topology, and pixel information. The focus of this work is on the classification of the major and branch arterial segments into LMA, LAD, LCX, diagonal branch (D1), obtuse marginal branch (OM1), and ramus intermedius branch (RI). We first extract the entire vascular tree from the ICAs using our previously designed feature pyramid U-Net++ (FP-U-Net++) [9]. After that, we generate the centerline of the whole vascular tree and find the key points to generate the vessel graph. Finally, we extract positional and topological features from vessel segments and perform semantic segmentation.

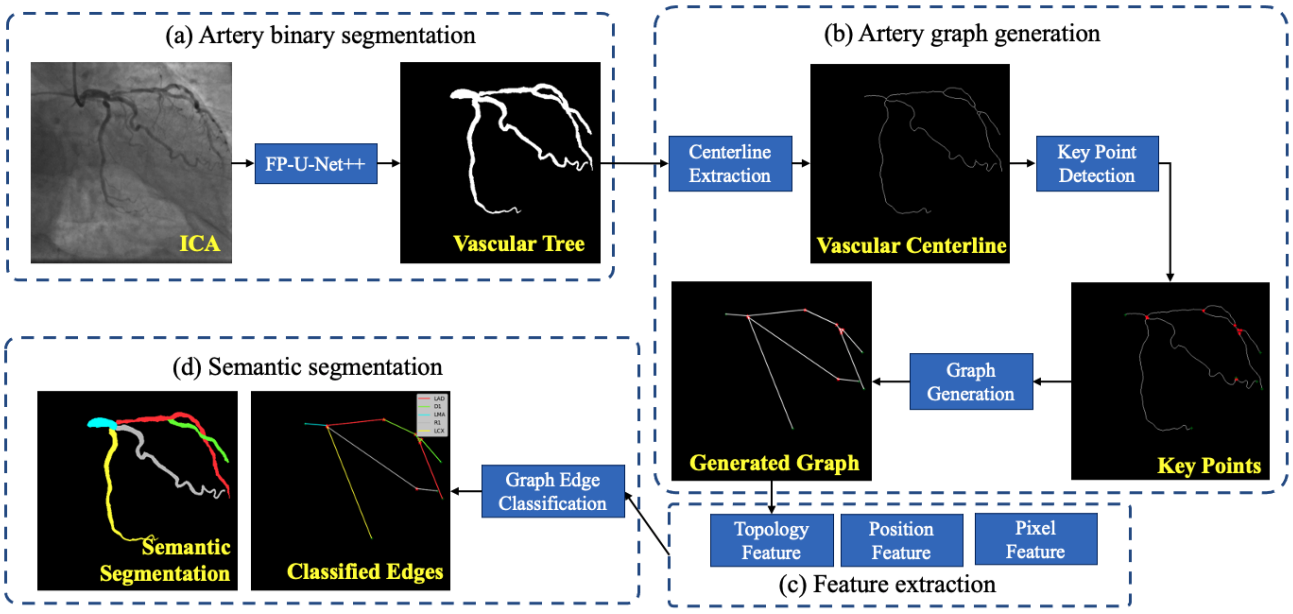

Figure 2: Workflow of coronary artery semantic segmentation. FP-U-Net++ is a deep learning-based neural network for coronary artery segmentation, published by Zhao *et al*. in [9].

2. Methods

2.1. Enrolled Subjects

This retrospective study enrolled 113 patients who received ICA from February 26, 2019, to July 18, 2019. The ethics committee approved of The First Affiliated Hospital of Nanjing Medical University. ICA was performed using an interventional angiography system (AXIOM-Artis, Siemens, Munich) and was acquired at 15 frames/sec at the Jiangsu Province People's Hospital, China. The image sizes of ICA videos ranged from 512×512 to 864×864, and the pixel spacing ranged from 0.2 mm to 0.39 mm.

The dataset consists of 225 left ventricle ICAs with 135 LAO images and 90 RAO images. For each patient, at most three standard views were selected, and then only one frame was selected from the view video for semantic segmentation. The vessel contours were manually drawn by well-trained operators, confirmed by an experienced interventional cardiologist, and then provided to this study as the ground truth. For each angiogram, we annotated LMA, LAD, LCX, D1, OM1, and RI arteries.

2.2. Artery Tree Segmentation

In general, current deep-learning-based models for medical image segmentation are variants of the encoder-decoder-based architecture, such as U-Net [13]. Many recent networks employed the classification network with the pre-trained weights from ImageNet [14] as the backbone of the encoder. In U-Net++, the skip connections are modified by using nested and dense connections [15]. In our latest paper [9], the multi-scale technique is improved by feature pyramids, which are built upon image pyramids and form a fundamental solution for utilizing features from different scales. To leverage the pyramid features of the hierarchy decoder in U-Net++, we resize the feature maps extracted from different layers and integrate them to generate the final feature map. By using pyramid features, the multi-scale problems are significantly resolved. The input of the network is the raw ICA, and the output is the binary mask of the entire vascular tree. To train the FP-U-Net++ network, we adopt a combined loss function with Dice loss, dilated loss, and L2 normalization, as shown in Eq. 1.

$$L_{loss} = \left(1 - \frac{2|\hat{y} \cap y|}{|\hat{y}| + |y|}\right) + \left(1 - \frac{2|d(\hat{y}) \cap d(y)|}{d(|\hat{y}|) + d(|y|)}\right) + ||W||_2 \quad (1)$$

where y is the ground truth for one pixel of the ICA and $\hat{y}$ is the model prediction. Our artery tree segmentation model achieved an average Dice score of 0.8899 [9]. Results from this binary segmentation model are used to generate the vascular centerline for coronary artery segment separation and semantic labeling.

2.3. Artery Graph Generation

The artery graph generation process includes centerline extraction and segment separation. Centerline extraction aims at removing the redundant pixels in the binary mask while preserving the topology and connectivity of the vascular tree. In our implementation, the centerline of the vascular tree is generated by using erosion and dilatation operations [16]. The morphological erosion algorithm with a kernel of 5×5 kernel is employed to remove the redundant pixels in the binary mask. The morphological dilation algorithm with a kernel of 3×3 is employed to preserve the connectivity of the vascular tree by expanding the eroded binary arterial tree. The extracted centerline is thus a representation of the vascular tree, which contains three types of nodes [17]: the degree-one nodes are the end of arteries, and the degree-two nodes are connecting points; the nodes whose degree is greater or equal to 3 are bifurcation points.

Each pixel in a centerline is iterated, and then the arterial nodes are extracted by finding the bifurcation and the endpoints. To find the links between the nodes, each pair of points are added to the graph if they are connected adjacently. After that, we remove the degree-two points and corresponding edges from the centerline to generate the undirect graph.

Each arterial segment is represented by a link between two nodes in the generated graph. Semantic segmentation will label the arteries by determining the type of each graph edge and assigning the arterial type to the arterial segment based on the pixel-level features between any of the two adjacent nodes [18] and the topology information.

In clinical practice, if the maximum diameter of the arterial segment is smaller than 1.8 mm, the cardiologist removes this artery segment due to low-level clinical significance for the following analysis [9]. In addition, any short arterial segments with less than 20 pixels in the centerline are also removed. The diameters of the arterial segments are calculated using the distance transform algorithm proposed by Maurer *et al*. [19].

2.4. Artery Feature Extraction and Segment Label Assignment

The basic idea of arterial semantic segmentation is to classify the segments into different classes of arteries. After that, we assign the arteries with different categorical labels to achieve semantic segmentation. As demonstrated in section 2.3, each artery segment is represented by a link between two nodes. We use the features extracted from this segment and its corresponding edge when we classify a specific segment. For feature extraction from the edge, topology information will be used: the degree of the nodes connected by this edge will be used as the feature. We also extract the position and pixel features from the segment (see Table **1**). Using the extracted features of each arterial segment, a machine learning classifier is employed to perform artery segment classification, and a grid search will be used to find the best classifier (see section 3). The semantic segmentation results are generated by classifying the arterial segments into different classes, and each segment is classified.

Table 1: List of features measured for each artery segment.

Type	Index	Feature Description
Pixel feature	1	Number of the pixels in the artery segment
	2	Length of the centerline in pixels
	3-6	Standard deviation, mean, the minimum and maximum radius of the artery segment
	7-8	Mean and standard deviation of the intensities within the artery segment
	9-10	Mean and standard deviation of the intensities within the centerline of the artery segment
Position feature	11-14	Weighted and absolute centers of the segment positions related to the center of the vascular tree
	15-22	Weighted and absolute positions of the two key points related to the vascular tree center
	23-30	Weighted and absolute positions of the two key points related to the artery segment center
Topology feature	31-32	Degree of the two key points
Projection view	33	1 represents the left anterior oblique view, and 0 is the right anterior oblique view

Each artery segment is classified into one of six types, including LMA, LAD, LCX, D1, OM1, and RI. At the training stage, the dataset was split into 70% subjects as a training set and the rest 30% as a test set. As a result, 158 and 67 images were grouped into the training set and test set, respectively. We employ a support vector machine (SVM) with kernel functions, random forest, and multiple layer perceptron (MLP) as the classifiers to perform the artery segment classification. All classifiers were implemented by Weka 3.8 [20]. A grid search is performed to find the optimal parameters. The settings of the grid search are shown in Table **2**.

Table 2: Settings of the grid search for artery.

Model	Parameter 1	Parameter 2
SVM	Kernel: RBF kernel, polynomial kernel, linear kernel	Regularization parameter: 0.01, 0.1, 1.0, 10, 100
Random Forest	Maximum depth: 5, 10, 15, 20	# Decision tree: [5, 10, 20, 50]
MLP	Learning rate: 0.1, 0.01, 0.001	Layer settings: [20], [20,10], [20,20,10], [30,30,20,10], [30,20,20], [30,20,20,10]

The overall workflow of the designed artery graph generation and semantic labeling algorithm is shown in Algorithm **1**.

2.5. Evaluation Metrics

Evaluation of artery segment classification: Artery segment classification is a multi-class classification task. The input is the extracted features from the artery segment, and the output is the probability distribution of the

Algorithm 1. Artery graph generation and semantic labeling.

Input:
I: ICA image; s: pixel size of the ICA

Output:
Semantic labels for artery pixels.

1. Extract ICA binary image using the trained FP-U-Net++ deep learning model;
2. Extract vascular centerline using morphological erosion and dilation algorithms;
3. Find the bifurcation points and end points to separate the vascular centerline into artery segments;
4. Calculate the diameters for each arterial segment;
5. Remove the artery segments with the maximum dimeter smaller than 1.8 mm;
6. Extract position, pixel and topological features listed in Table 1 for each arterial segment;
7. Classify arterial segment using the trained machine learning classifier for semantic labeling;
8. Assign the semantic label, which is the predicted class, to each pixel in this arterial segment.

artery class among six types. The class with the maximum probability is regarded as the classification result. We evaluated the performance using average accuracy (ACC), sensitivity (SN), and specificity (SP). The SN measures the proportion of the true positive samples that are correctly predicted, while the SP indicates the proportion of the true negative samples that are correctly predicted. An ACC, SN, or SP of 1 implies a perfect prediction. The definitions of average ACC, SN and SP are shown in Eq. 2 to 4.

$$average\_ACC = \frac{1}{n}\sum_{c=1}^{C}\frac{TP_c + TN_c}{TP_c + TN_c + FN_c + FP_c} \tag{2}$$

$$average\_SN = \frac{1}{n}\sum_{c=1}^{C}\frac{TP_c}{TP_c + FN_c} \tag{3}$$

$$average\_SP = \frac{1}{n}\sum_{c=1}^{C}\frac{TN_c}{TN_c + FP_c} \tag{4}$$

where C is the number of classes in the dataset; TP_c is the number of the true positive arterial segments classified into arterial type c. TN, FN, and FP represent true negative, false negative, and false positive. In our experimental setting, C equals 6, which indicates there are 6 types of arterial segments.

Evaluation of artery semantic segmentation: Semantic segmentation is to assign labels for each pixel in the image. We evaluated the semantic segmentation performance using ACC and mean Intersection over Union (mIoU). IoU measures the proportion of the intersection between the segmented pixels and the pixels in the ground truth over the number of pixels in either the segmented pixels or the ground truth. The definition of mIoU is shown in Eq. 5.

$$mIoU = \sum_{c=1}^{C}\frac{|\widehat{y_c} \cap y_c|}{|\widehat{y_c}| + |y_c|} \tag{5}$$

where C is the number of arterial classes, $\widehat{y_c}$ represents the predicted arterial mask for class c, and y_c indicates the ground truth of the coronary artery.

3. Results

3.1. Results of Artery Graph Generation

We first applied our binary artery segmentation model [9] to our dataset to generate the coronary artery binary mask. Then we extracted the centerlines and generated a graph for each ICA. The edge linking algorithm was applied to obtain the topology structure and separate the vascular tree into different arterial segments [21].

In Fig. **3** (c), the bifurcation points and endpoints are annotated by red stars and green plus. The coronary artery segments were obtained by splitting the vascular tree according to the detected key points. Cardiologists only focus on the main arterial branches in clinical practice, and the branches with limited lengths are ignored. In our implementation, if the length of the centerline is less than 20 pixels, then it was removed. As a result, in the training set and the test set, 1609 and 729 segments were extracted, respectively.

3.2. Results of Artery Semantic Segmentation

The features extracted from the artery segments were scaled using z-score normalization. We performed the grid search shown in Table **2**. The arterial segments were used for model training, and the performance was reported according to the prediction on the test set. The random forest achieved its best performance with 20 decision trees for ensemble, and the depth for each tree was 5; for MLP, the model achieved the best performance with a learning rate of 0.1 and a layer with 20 hidden units, which indicated that there was only one layer with 20 neurons; for the SVM, the model achieved the best performance with a regulation parameter of 10.0 and an RBF kernel function. The performance of the best classifiers is shown in Table **3**. We also evaluated the results using image semantic segmentation metrics. The performance is reported in Table **4**.

Table 3: Grid search results for coronary artery segment classification. The highest evaluation metrics are marked in bold.

Model	ACC	SN	SP
RF	0.6498	0.6077	0.5929
MLP	0.6475	0.5982	0.5789
SVM	**0.7033**	**0.6623**	**0.6437**

Table 4: Evaluation for coronary artery semantic segmentation. The highest evaluation metrics are marked in bold.

Metrics	Model	LMA	LAD	LCX	D1	OM1	RI	Mean
ACC	RF	**0.9015**	0.8004	0.6211	0.5160	**0.5912**	0.8059	0.6137
	MLP	0.8855	0.7865	0.6751	0.5281	0.5213	0.8093	0.6235
	SVM	0.8771	**0.8398**	**0.7461**	**0.6328**	0.5168	**0.8235**	**0.7076**
IoU	RF	**0.8585**	0.6039	0.5345	0.3384	**0.4187**	0.7910	0.6373
	MLP	0.8362	0.6370	0.5372	0.3861	0.3876	0.7198	0.6438
	SVM	0.8569	**0.6796**	**0.6014**	**0.4832**	0.4037	**0.8235**	**0.6868**

According to Table **3**, our approach achieved an average accuracy of 0.7033 for coronary artery segment classification. The SVM classifier outperformed other classifiers significantly in ACC, SN, and SP. According to Table **4**, the proposed approach achieved an accuracy of 0.7076 for pixel classification and 0.6868 for artery semantic segmentation. In Fig. **3**, we visualized the results generated for LAO and RAO views at each step.

4. Discussion

4.1. Performance Analysis for Artery Semantic Segmentation

In this paper, a new machine learning-based algorithm was applied to perform coronary artery segment classification. The SVM achieved an ACC of 0.7033, an SN of 0.6623 and an SP of 0.6437 among 729 arterial segments in the test set. The handcraft features only contained the low-level image feature and low-level position features, which limited the model performance. In addition, the number of training samples is not enough, further studies should increase training samples.

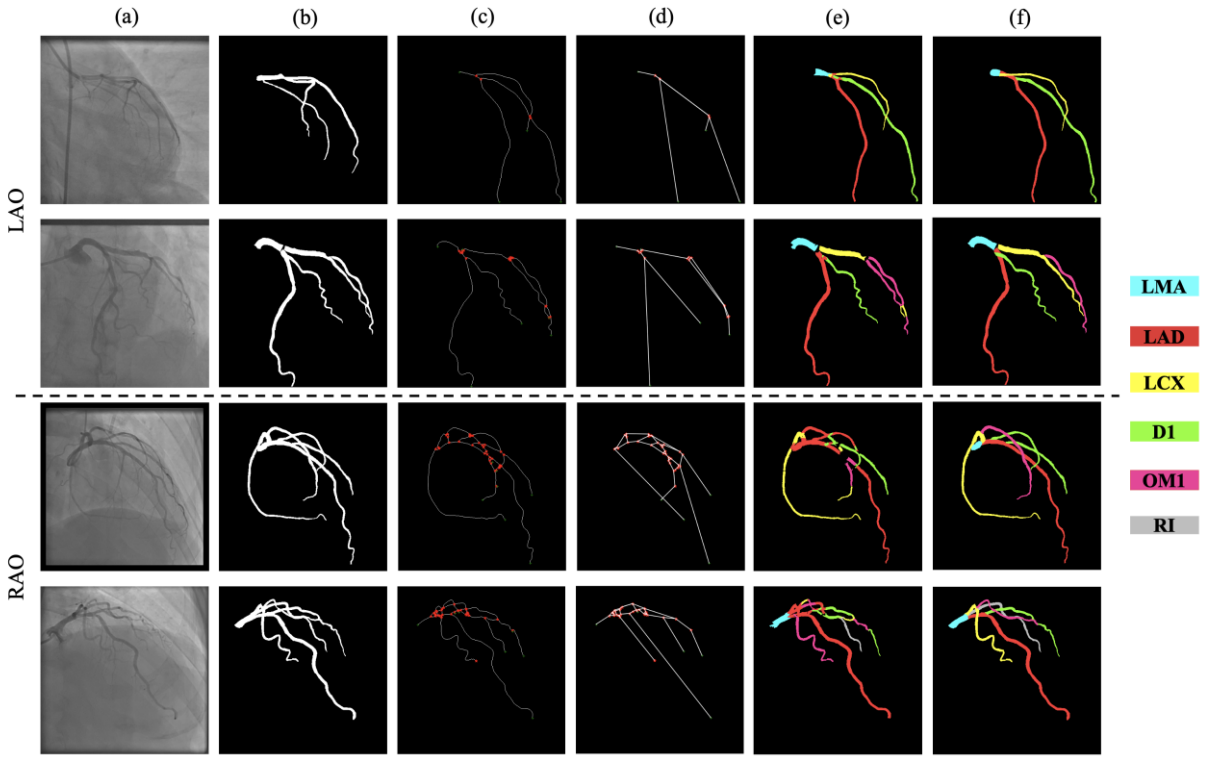

Figure 3: Experimental results on LAO (top) and RAO (bottom) subsets of (a) original ICAs; (b) artery binary segmentation masks; (c) generated coronary centerline and detected key points, where red points indicate bifurcation points and green points are endpoints; (d) generated artery graph for topological feature extraction; (e) semantic segmentation predictions; and (f) semantic segmentation ground truth. LMA, left marginal artery; LAD, left anterior descending; LCX, left circumflex artery; D1, diagonal branch one; OM1, obtuse marginal branch one; RI, ramus intermedius branch.

For semantic segmentation, the proposed approach achieved a mIoU of 0.6868 and an average pixel classification accuracy of 0.7076. According to the grid search and the performance reported in Table **4**, the SVM with an RBF kernel function significantly outperformed the random forest and MLP in ACC and mIoU.

For the proposed approach, errors come from two parts: (1) the coronary artery segments removed due to the limited length, and (2) the mapping method between the centerline and the coronary segment. For the first reason, in our implementation, if the length of the centerline is smaller than a 20-pixel length, then it was removed. However, the removed artery segments were incorrectly measured when evaluating the semantic segmentation performance, which degraded the model performance. For the second reason, the function for mapping the coronary centerline and segment cannot guarantee a perfect match. In our implementation, we first interpolated the centerline by applying one-dimensional constant interpolation within the coordinate sequence of the centerline pixels. Then a perpendicular line was calculated for each interpolated coordinate. If the perpendicular line containing the pixels belonged to the artery in the binary mask, then the pixel was mapped to the centerline. By iterating all the interpolated coordinates in the artery centerline, the arterial pixels were partitioned to the arterial segment. However, the pixels near the bifurcation key points cannot be correctly mapped to the centerline caused by the overlap of the generated perpendicular lines and two-dimensional projection views. These errors may be resolved from different frames and views by operators.

4.2. Clinical Overview and Application

ICA best assesses anatomic delineation of coronary arteries for clinical decisions due to its high spatial resolution and its real-time image acquisition. In clinical practice, an automated system for decision support of CAD diagnosis and treatment would require automated anatomical labeling of the coronary artery tree extracted from ICA. This automated process can be achieved with higher efficiency and reproducibility by performing semantic segmentation.

5. Conclusion

We propose a machine learning-based approach to classify individual coronary arteries in ICAs by incorporating global position, topology information, and pixel-level intensity. Our previously developed binary segmentation network was employed to generate the arterial binary mask to precisely extract the entire vascular tree. By generating the centerline of the vascular tree, we identified the key points and converted the centerlines into an artery graph. An edge in the graph represents each artery segment. Finally, we extracted 33 handcraft features of the artery segment, employed an SVM classifier to classify the artery segments, and further generated the semantic segmentation results. The proposed approach achieved an accuracy of 70.33% for the multi-class artery segment classification and a mean intersection over union of 0.6868 for artery semantic segmentation. It shows promise for clinical use to improve efficiency and reproducibility in a cath lab.

Acknowledgments

This research was supported by a new faculty startup grant from Michigan Technological University Institute of Computing and Cybersystems (PI: Weihua Zhou) and a seed grant from Michigan Technological University Health Research Institute.

Conflict of Interest

The authors declare no conflicts of interest.

References

[1] Benjamin EJ, Muntner P, Alonso A, Bittencourt MS, Callaway CW, Carson AP, Chamberlain AM, Chang AR, Cheng S, Das SR. Heart disease and stroke statistics-2019 update: a report from the American Heart Association. Circulation. Am Heart Assoc; 2019; 139(10): e56-e528.

[2] Boden WE, O'Rourke RA, Teo KK, Hartigan PM, Maron DJ, Kostuk WJ, Knudtson M, Dada M, Casperson P, Harris CL, Chaitman BR, Shaw L, Gosselin G, Nawaz S, Title LM, Gau G, Blaustein AS, Booth DC, Bates ER, Spertus JA, Berman DS, Mancini GBJ, Weintraub WS. Optimal Medical Therapy with or without PCI for Stable Coronary Disease. N Engl J Med. 2007 Apr 12; 356(15): 1503-1516. https: //doi.org/10.1056/NEJMoa070829

[3] Wu D, Wang X, Bai J, Xu X, Ouyang B, Li Y, Zhang H, Song Q, Cao K, Yin Y. Automated anatomical labeling of coronary arteries via bidirectional tree LSTMs. Int J Comput Assist Radiol Surg. 2019 Feb 1; 14(2): 271-280. https: //doi.org/10.1007/s11548-018-1884-6

[4] Gifani P, Behnam H, Shalbaf A, Sani ZA. Automatic detection of end-diastole and end-systole from echocardiography images using manifold learning. Physiol Meas. IOP Publishing; 2010; 31(9): 1091. https: //doi.org/10.1088/0967-3334/31/9/002

[5] Yang G, Broersen A, Petr R, Kitslaar P, de Graaf MA, Bax JJ, Reiber JHC, Dijkstra J. Automatic coronary artery tree labeling in coronary computed tomographic angiography datasets. 2011 Comput Cardiol. 2011. p. 109-112.

[6] Nasr-Esfahani E, Karimi N, Jafari MH, Soroushmehr SMR, Samavi S, Nallamothu BK, Najarian K. Segmentation of vessels in angiograms using convolutional neural networks. Biomed Signal Process Control. 2018 Feb; 40: 240-251. https: //doi.org/10.1016/j.bspc.2017.09.012

[7] Nasr-Esfahani E, Samavi S, Karimi N, Soroushmehr SR, Ward K, Jafari MH, Felfeliyan B, Nallamothu B, Najarian K. Vessel extraction in X-ray angiograms using deep learning. 2016 38th Annu Int Conf IEEE Eng Med Biol Soc EMBC. IEEE; 2016. p. 643-646. https: //doi.org/10.1109/EMBC.2016.7590784

[8] Iyer K, Najarian CP, Fattah AA, Arthurs CJ, Soroushmehr SM, Subban V, Sankardas MA, Nadakuditi RR, Nallamothu BK, Figueroa CA. Angionet: a convolutional neural network for vessel segmentation in X-ray angiography. Sci Rep. Nature Publishing Group; 2021; 11(1): 1-13. https: //doi.org/10.1038/s41598-021-97355-8

[9] Zhao C, Vij A, Malhotra S, Tang J, Tang H, Pienta D, Xu Z, Zhou W. Automatic extraction and stenosis evaluation of coronary arteries in invasive coronary angiograms. Comput Biol Med. 2021; 136: 104667. https: //doi.org/10.1016/j.compbiomed.2021.104667

[10] Zhai M, Du T, Yang R, Zhang H. Coronary Artery Vascular Segmentation on Limited Data via Pseudo-Precise Label. 2019 41st Annu Int Conf IEEE Eng Med Biol Soc EMBC. 2019. p. 816-819. https: //doi.org/10.1109/EMBC.2019.8856682

[11] Xian Z, Wang X, Yan S, Yang D, Chen J, Peng C. Main Coronary Vessel Segmentation Using Deep Learning in Smart Medical. Huang C, editor. Math Probl Eng. 2020 Oct 21; 2020: 1-9. https: //doi.org/10.1155/2020/8858344

[12] Yang S, Kweon J, Roh J-H, Lee J-H, Kang H, Park L-J, Kim DJ, Yang H, Hur J, Kang D-Y, Lee PH, Ahn J-M, Kang S-J, Park D-W, Lee S-W, Kim Y-H, Lee CW, Park S-W, Park S-J. Deep learning segmentation of major vessels in X-ray coronary angiography. Sci Rep. 2019 Dec; 9(1): 16897. https: //doi.org/10.1038/s41598-019-53254-7

[13] Ronneberger O, Fischer P, Brox T. U-net: Convolutional networks for biomedical image segmentation. Int Conf Med Image Comput Comput-Assist Interv. Springer; 2015. p. 234-241. https: //doi.org/10.1007/978-3-319-24574-4_28

[14] Deng J, Dong W, Socher R, Li L-J, Li K, Fei-Fei L. Imagenet: A large-scale hierarchical image database. 2009 IEEE Conf Comput Vis Pattern Recognit. Ieee; 2009. p. 248-255. https: //doi.org/10.1109/CVPR.2009.5206848

[15] Zhou Z, Rahman Siddiquee MM, Tajbakhsh N, Liang J. Unet++: A nested u-net architecture for medical image segmentation. Deep Learn Med Image Anal Multimodal Learn Clin Decis Support. Springer; 2018. p. 3-11. https: //doi.org/10.1007/978-3-030-00889-5_1

[16] Edward D. An Introduction to Morphological Image Processing | (1992) | Dougherty | Publications | Spie [Internet]. [cited 2022 May 16]. Available from: https: //spie.org/Publications/Book/48126?SSO=1

[17] Xie J, Zhao Y, Liu Y, Su P, Zhao Y, Cheng J, Zheng Y, Liu J. Topology reconstruction of tree-like structure in images via structural similarity measure and dominant set clustering. Proc IEEECVF Conf Comput Vis Pattern Recognit. 2019. p. 8505-8513. https: //doi.org/10.1109/CVPR.2019.00870

[18] Dashtbozorg B, Mendonça AM, Campilho A. An automatic graph-based approach for artery/vein classification in retinal images. IEEE Trans Image Process. IEEE; 2013; 23(3): 1073-1083. https: //doi.org/10.1109/TIP.2013.2263809

[19] Maurer CR, Qi R, Raghavan V. A linear time algorithm for computing exact Euclidean distance transforms of binary images in arbitrary dimensions. IEEE Trans Pattern Anal Mach Intell. IEEE; 2003; 25(2): 265-270. https: //doi.org/10.1109/TPAMI.2003.1177156

[20] Hall M, Frank E, Holmes G, Pfahringer B, Reutemann P, Witten IH. The WEKA data mining software: an update. ACM SIGKDD Explor Newsl. ACM New York, NY, USA; 2009; 11(1): 10-18. https: //doi.org/10.1145/1656274.1656278

[21] Kovesi PD. MATLAB and Octave functions for computer vision and image processing. Cent Explor Target Sch Earth Environ Univ West Aust Available https: //www.peterkovesi.com/matlabfns/. 2000; 147: 230.